The effect of a tall tower on flow and dispersion through a model urban neighborhood

Part 2. Pollutant dispersion

Laurie A. Brixey,[a] Jennifer Richmond-Bryant,[b] David K. Heist,[c] George E. Bowker,[d] Steven G. Perry[c] and Russell W. Wiener[e]

[a]Alion Science and Technology, P.O. Box 12313, Research Triangle Park, NC 27709, USA

[b]Environmental and Occupational Health Sciences, Hunter College, City University of New York, 425 East 25th Street, New York, NY 10010, USA

[c]Atmospheric Sciences Modeling Division, Air Resources Laboratory, National Oceanic and Atmospheric Administration, Research Triangle Park, NC 27711, USA

[d]Atmospheric Modeling Division, National Exposure Research Laboratory, US Environmental Protection Agency, Research Triangle Park, NC 27711, USA

[e]National Homeland Security Research Center, US Environmental Protection Agency, Research Triangle Park, NC 27711, USA

Disclaimer

The research presented here was performed under the Memorandum of Understanding between the U.S. Environmental Protection Agency (EPA) and the U.S. Department of Commerce's National Oceanic and Atmospheric Administration (NOAA) and under agreement number DW13921548. This work constitutes a contribution to the NOAA Air Quality Program. Although it has been reviewed by EPA and NOAA and approved for publication, it does not necessarily reflect their policies or views. Mention of trade names or commercial products does not constitute endorsement or recommendation for use.

Abstract

This article is the second in a two-paper series presenting results from wind tunnel and computational fluid dynamics (CFD) simulations of flow and dispersion in an idealized model urban neighborhood. Pollutant dispersion results are presented and discussed for a model neighborhood that was characterized by regular city blocks of three-story row houses with a single 12-story tower located at the downwind edge of one of these blocks. The tower had three

significant effects on pollutant dispersion in the surrounding street canyons: drawing the plume laterally towards the tower, greatly enhancing the vertical dispersion of the plume in the wake of the tower, and significantly decreasing the residence time of pollutants in the wake of the tower. In the wind tunnel, tracer gas released in the avenue lee of the tower, but several blocks away laterally, was pulled towards the tower and lifted in the wake of the tower. The same lateral movement of the pollutant was seen in the next avenue, which was approximately 2.5 tower heights downwind of the tower. The tower also served to ventilate the street canyon directly in its wake more rapidly than the surrounding areas. This was evidenced by CFD simulations of concentration decay where the residence time of pollutants lee of the 12-story tower was found to be less than half the residence time behind a neighboring three-story building. This same phenomenon of rapid vertical dispersion lee of a tower among an array of smaller buildings was also demonstrated in a separate set of wind tunnel experiments using an array of cubical blocks. A similar decrease in the residence time was observed when the height of one block was increased.

Introduction

As part of an effort to protect the health of the population from releases of pollutants and other toxic substances into the atmosphere, it is essential to be able to predict, evaluate, and understand airflow patterns and dispersion of pollutants within populated areas. Pollution can originate from a routine source, such as traffic, or from an accidental or even intentional release of hazardous material. In the latter case, an understanding of the area experiencing harmful levels can be vital for protecting and saving lives. Many studies have shown the negative health impacts that pollutants in urban areas (such as particulate matter, nitrogen dioxide, sulfur dioxide, carbon monoxide, and ozone) have on the population and the economic cost of traffic-related pollution on human health.[1–6] In addition, the importance of understanding exposure in urban areas is magnified by the high population densities.

Understanding exposure can be particularly difficult for urban and suburban locations due to the complexity of the airflow patterns within the building canopy and the diversity of pollutant sources and locations. These factors create a myriad of poorly described exposure microenvironments within the domain, further confounded by the often inadequate representations of the pollution sources within the domain.

This article is part of a larger series of papers related to the Brooklyn Traffic Real-Time Ambient Pollutant Penetration and Environmental Dispersion (B-TRAPPED) Study field work.[7–13] These papers present the results of an intensive study that comprises field measurements, physical modeling, and computer simulations of the airflow and pollutant dispersion patterns within an urban neighborhood in Brooklyn, NY, composed of three-story attached row houses, one 12-story building, and a major expressway.

Here we present the results from studies of pollutant dispersion for an idealized scale model of the Brooklyn neighborhood using two systems: a meteorological wind tunnel (MWT) and computational fluid dynamics (CFD) modeling. A companion paper[11] describes the flow patterns in the same two systems. The MWT and CFD studies were designed to be complementary, with the goals being (1) to identify important flow and dispersion patterns, (2) to determine the effect of the tall building on the dispersion patterns within the neighborhood, and (3) to determine the residence time in the street canyon downwind of the tower and determine whether it is significantly different from the street canyon residence time downwind of a shorter building. Additionally, knowledge of the locations where pollutant concentrations are high provides insight into potential exposures.

Wind tunnel studies are important tools for understanding flow and pollutant dispersion and for developing and evaluating numerical models because wind tunnels account for the primary physical processes and provide a relatively constant and controlled environment where a high density of repeatable measurements can be made.[14] Among the most physically realistic numerical models are CFD codes. They are useful tools for investigating the same phenomena at very high temporal and spatial resolution and can be run for a large number of environmental conditions. Consequently, they are being used increasingly in the study of the urban environment.[15–26]

A number of wind tunnel and CFD studies have investigated two-dimensional street canyons with buildings of equal height.[16,27,28] Xia and Leung[27] showed that for buildings of equal height contaminants were mostly confined within the counterclockwise vortex formed in the street canyon with little escaping above the rooflines of the buildings. Liu *et al.*[16] concluded that more than 95% of the pollutant remained inside the street canyons examined. Meroney *et al.*[28] found that within an urban boundary layer pollutants were almost entirely trapped in street canyons with equal upwind and downwind building heights.

Two-dimensional street canyons with the upwind building taller than the downwind building have been investigated using CFD simulations.[22,27] So *et al.*[22] found that the taller upwind building caused reentrainment of downstream flow back into the canyon, facilitating the circulation and export of pollutants. Dilution of the pollutants was also increased by the mixing of canyon vortices. Xia and Leung[27] found that particles released into a two-dimensional street canyon with taller upwind buildings were more well mixed in the street canyon, and more particles escaped from the street canyon, when compared to scenarios with a taller downwind building or buildings of equal height. Perry *et al.*[29] describe flow in a three-dimensional wind tunnel model of lower Manhattan and saw significant upwash in the lee of tall buildings in the model.

For the wind tunnel and CFD studies presented here, the Brooklyn neighborhood was modeled as an array of city blocks made up of contiguous row houses of uniform height, having common backyards that form closed courtyards. One notable exception to the otherwise uniform-height row houses within the study neighborhood is a 12-story building (tower) located immediately upwind of the major source street. Based on the previous studies of urban flow cited above, the isolated tower in the Brooklyn neighborhood was expected to have a significant influence on airflow and dispersion patterns and therefore was included in these idealized models.

This paper describes the equipment and methods used for the wind tunnel study as well as details of the CFD model and methods. We also present and compare time-averaged concentration results from the wind tunnel and CFD studies of dispersion in the urban neighborhood model and discuss the impact that the single tall tower had on the concentration fields. Additionally, concentration decay simulations from the CFD study of the urban neighborhood are compared with wind tunnel concentration-decay observations in an array of cubical blocks. A discussion of residence time of pollutants in the street canyon is also included.

Methods

Wind tunnel methods

The equipment and methods described here were used for the wind tunnel measurements of pollutant concentration. Details of the urban neighborhood model and time-averaged concentration measurement method are included in our discussion. We also briefly describe a

separate wind tunnel model involving cubical blocks and a time-dependent concentration measurement method.

Meteorological wind tunnel. A scale model of the urban neighborhood was placed within the MWT at the U.S. Environmental Protection Agency's Fluid Modeling Facility and subjected to a scaled, neutral atmospheric boundary layer. The simulated atmospheric boundary layer was generated by tripping the otherwise straight-line flow with three truncated triangular Irwin spires[30] mounted near the entrance to the test section (3.7 m wide, 2.1 m high, and 18.3 m long) followed by a regular staggered array of roughness blocks (1.9 cm high, 2.8 cm long, and 2.8 cm wide) covering 25% of the floor area within the test section. More details on the development of the boundary layer are provided in Heist *et al.*[11]

The boundary layer was characterized using the standard logarithmic profile as follows:

$$\frac{U(z)}{u^*} = \frac{1}{\kappa}\ln\left(\frac{z-d}{z_0}\right), \tag{1}$$

where U is the mean velocity as a function of height (z), u^* is the friction velocity, κ is von Karman's constant (taken to be 0.4), z_0 is the roughness length scale, and d is the displacement height. The values for the boundary layer were estimated from mean flow measurements to be $u^* = 0.23$ m s^{-1}, $z_0 = 0.07$ cm (7 cm full scale), and $d = 0$.

Idealized urban neighborhood model. The geometry of the urban neighborhood model was based on dimensions consistent with locations found in Brooklyn, NY, USA. Typically, these neighborhoods consist of attached row houses of similar heights forming a rectangular city block. The row houses have adjoining backyards that form an open area, or courtyard, in the center of each block. The domain modeled within the wind tunnel at a scale of 1:100 consisted of a total of 30 simplified city blocks. The distribution and size of the blocks are shown in Fig. 1. The scaled heights of the blocks were 12 cm (H), approximately corresponding to three-story buildings. The streamwise "streets" were 1H wide while the cross-stream "avenues" were 2H wide. The only exception was the cross-stream avenue containing the line source, which was 2.67H wide, corresponding to the width of a major urban multi-lane expressway. A tall tower of height 4H (12 stories full scale) was included in the model and is shown as the cross-hatched area in Fig. 1 (column 2, row D). This corresponds to a similar isolated tall building along the major thoroughfare in the Brooklyn neighborhood. All positions within the model were referenced to a coordinate system with its origin on the tunnel floor, centered laterally in the

tunnel and at the alongwind source location within the central street canyon (see Fig. 1, Avenue B).

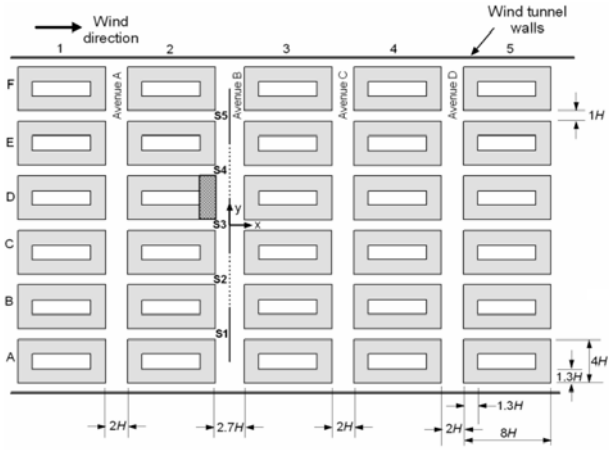

Fig. 1 Model layout in the MWT. Cross-hatching indicates location of tower.

Time-averaged concentration measurements. To simulate the pollution released by traffic along the expressway, a line source emitting ethane tracer gas (C_2H_6, minimum purity 99.5 mole percent) was placed along the axis of Avenue B (Fig. 1). The ethane tracer used in this study has a molecular weight (MW) of 30 and is only slightly heavier than air (MW of 29). In combination with the high turbulence level at the release points and a net release rate of 3.0 L min^{-1}, this tracer may be regarded as neutrally buoyant.

The line source was constructed of a brass tube (0.8 cm diameter) with small (0.07 cm diameter) holes drilled every 1 cm in a row on the underside of the tube. The tube was 60 cm in length with the ends capped and was placed 1 cm off the floor of the tunnel with the row of holes facing the floor of the tunnel to minimize any momentum jetting as the ethane was introduced. A nearly neutrally buoyant release with minimal positive vertical momentum resulted in insignificant source-induced plume rise.

Vertical concentration profiles were measured by collecting samples through 0.16 cm (inner diameter) tubes that were arranged in a group of six on a vertical sampling rake attached to the automated carriage system in the wind tunnel. The samples were drawn through flame ionization detectors (FIDs, Model 400A, Rosemount Analytical, Solon, OH, USA) operating in the continuous sampling mode for analysis. Sampling duration was 120 s, and the output signals from the analyzers were digitized at the rate of 20 Hz and processed on a personal computer.

To compare wind tunnel data to the CFD results, the measured concentrations were non-dimensionalized to account for differences in scale, wind speed, and source strength. The non-dimensional concentration for the finite line source, χ_{fls}, is defined as

$$\chi_{fls}(x,y,z) = \frac{C(x,y,z)U_o H}{Q/L_y}, \tag{2}$$

where $C(x,y,z)$ is the measured concentration, U_0 is the freestream velocity (4.2 m s^{-1}), and Q/L_y is the source strength for a finite line source of length L_y.[14,28,31,32]

Comparison of the wind tunnel results to the CFD simulations required calculation of the result of a continuous "infinite" line source, stretching across the width of the measurement domain, using the data obtained for the individual line source segments. For each experiment, the finite line source was placed in one of five source positions (S1 through S5, as indicated in Fig. 1), and concentration measurements were made throughout the domain. Then, the line source was moved laterally along the release avenue by one block, and the measurements were repeated. The result for an "infinite" line source was calculated by reflecting, superimposing, and summing concentration results from the individual line source segments, accounting for inherent symmetries in the model domain as follows:

$$\chi(x,y,z) = \sum_{i=-\infty}^{\infty} \chi_{fls}(x, y + iL_y, z), \tag{3}$$

where $\chi(x,y,z)$ is the predicted concentration from an infinite line source and χ_{fls} is the normalized measured concentration based on a finite line source of width L_y. Due to the fact that the model is symmetric along the x-axis around the center of the tower, measurements were only made for source locations S1, S2, and S3. It is reasonable to assume that the results from source location S4 would be a reflection of source S3 and, likewise, S5 would be a reflection of S2. This is supported by the symmetry around the tower of velocity vectors measured in the wind tunnel model, which are presented in Heist *et al.*[11] and flow visualization observations not reported here.

Cubical block array model. For the purpose of comparison with the concentration decay studies from the CFD modeling, results will be presented from transient, or time-dependent, wind tunnel measurements of concentration decay in an array of cubical blocks with dimensions of 15 cm.[33] Concentration decay measurements were not performed in the wind tunnel for the

idealized urban neighborhood model shown in Fig. 1. The transient wind tunnel experiments using the cubical block array are briefly described here.

The blocks were arranged in a regular matrix with spacing in both the windward and lateral directions equal to 15 cm. There were seven rows of blocks (11 buildings in each row) across the test section, perpendicular to the approach flow as depicted in Fig. 2. The height of the center block in the third row was increased by placing additional blocks on top of it. Four different block heights were used in this study, 1*H* (15 cm), 1.5*H*, 2*H*, and 3*H*, with a freestream wind speed of 4.2 m s^{-1}.

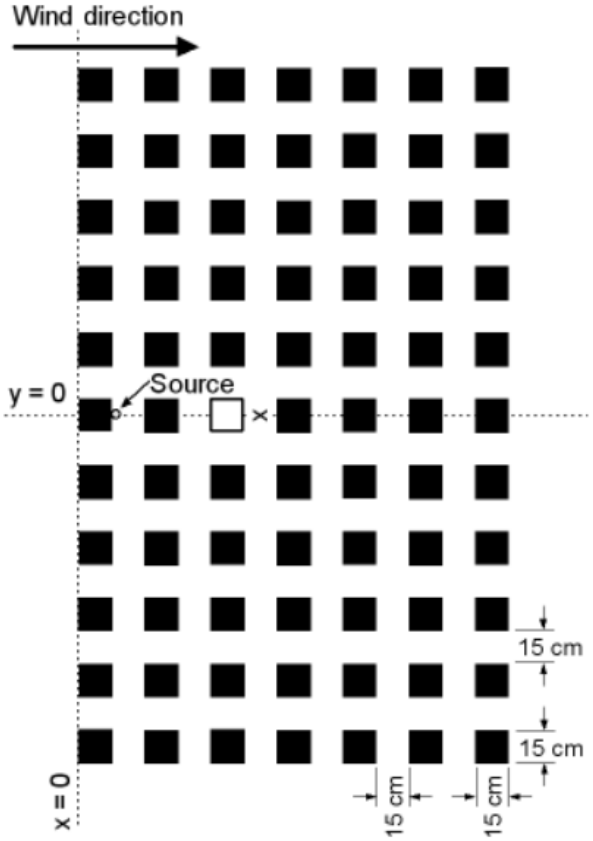

Fig. 2 Model layout for the cubical blocks study of concentration decay in the MWT. The sampling point is indicated by an x. The height of the white block was varied for the study.

Concentration decay measurements. Ethane tracer gas was released near the floor of the wind tunnel 1 cm downwind of the center block in the first row. A single sampling tube was positioned 7.5 cm downwind of the center block in the third row (the block of varying height). Tracer gas concentration was measured using a single FID operating in the continuous sampling

mode. Time traces were recorded using LabView software (National Instruments, Austin, TX, USA) with data acquisition at 100 Hz. Forty separate tests were run for each of the four upwind block height scenarios. Data acquisition began 1 min after turning on the source (to allow the system to come to steady-state conditions). The source was shut off after 20 s of steady-state sampling, and data acquisition continued for an additional 20 s. The results of the 40 individual runs were averaged and used to calculate the residence time in the wake of the block of varying height.

Numerical modeling methods

Airflow modeling. Computer simulations of flow and dispersion patterns for the site were made using the FLUENT CFD software (FLUENT, Inc., Lebanon, NH, USA). A complete description of the airflow modeling and mesh characteristics is provided in Heist *et al.*[11] For the convenience of the reader, the main points are summarized here. Large eddy simulation (LES) was employed to capture the rapidly varying, large-scale fluid motion through the solution of the time-dependent turbulent Navier-Stokes equations. The simulation was implemented with a finite volume method.

A tetrahedral mesh with 2,029,900 elements was employed in the simulation. Two time-step refinements led to use of $\Delta t = 0.05$ s in the airflow simulation. A complete description of the airflow modeling and mesh refinement procedure is provided in Heist *et al.*[11] A logarithmic upstream velocity profile was used in the simulation to match that of the wind tunnel simulations (see eqn. (1)), with $u^* = 0.23$ m s^{-1}, $\kappa = 0.4$, $z_0 = 0.07$ m, and $d = 0$ m. All solid entities, including the building surfaces and ground, had no-slip and no-flow designations to preserve mass balance.

Model geometry. The CFD model geometry shown in Fig. 3 was created using the GAMBIT v.2.1.0 (FLUENT, Inc.) software. The model geometry was similar to that used in the wind tunnel, but some changes were made to accommodate memory constraints imposed by the meshing process. The model geometry consisted of three rows of the simplified city blocks with four blocks in each row. The first and second rows were separated by a distance of 3H, where H = 12 m. The second and third rows were separated by a distance of 2H, and the side streets had a width of 1H. A tower with a height of 4H (from the ground) was located in the third building from the left and upstream of the 3H-wide canyon, as shown in Fig. 3. $x = 0H$ was designated 1.67H downstream of the first row of buildings, $y = 0H$ was positioned at the center of the

domain between the second and third building columns, and $z = 0H$ was located at the ground. The domain limits were $-23.67H < x < 33.67H$, $-19H < y < 19H$, $0H < z < 8H$.

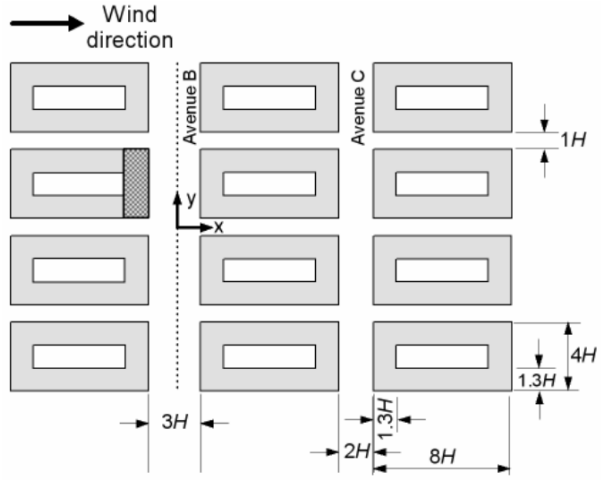

Fig. 3 CFD model layout for the urban neighborhood. Cross-hatching indicates location of tower.

Particle tracking. The line source along which particles were released was located along the central axis of Avenue B ($x = 0H$), spanning the width of the building array. One hundred massless tracer particles were released at every fluid time step (Δt) and tracked as they moved through the domain. Particles were released each fluid time step because the error in the particle simulation was limited by that of the fluid simulation. Lagrangian particle tracking was implemented with the solution of the drag equation for particle motion:

$$\frac{du_p}{dt} = \frac{1}{\tau_p}\left(u - u_p\right), \tag{4}$$

where u_p is particle velocity, t is time, and τ_p is particle relaxation time. Because a time-dependent airflow solution was implemented, u_p was updated after u was computed through the LES at each time step. Because the subgrid-scale turbulence model in the LES captured small-scale turbulence, the computed value of u included both the mean and fluctuating portions of the air velocity.

Concentration field. Two types of simulations were run to gather information about the concentration field characteristics. First, time-averaged concentration was calculated to study the spatial distribution of the concentration field. Second, the residence time behavior was tested by turning off the particle source. During each time step, particle concentration was computed in

each cell. Particle number concentration in each cell i, C_i, was adapted from Heinsohn's[34] formula for particle mass transport through a defined region of air:

$$C_i = \frac{n_i}{V_c}, \tag{5}$$

where V_c is volume of one cell (equal for all cells) and n_i is number of particles in the i^{th} concentration cell. Particle concentration was computed using an in-house FORTRAN95 code that used input from particle trajectory files generated by FLUENT. The concentrations in each cell were averaged over a 120 s time period.

To compute concentration, the domain was subdivided into 461,376 cubes with dimension $\frac{1}{3}H \times \frac{1}{3}H \times \frac{1}{3}H$. For clarification, it should be emphasized that this is a different grid from that used in the airflow simulations. Because the tetrahedral grid used in the LES was nonuniform, identification of cell location and estimation of cell volume would be too uncertain with the airflow solution mesh. Cell size was chosen to prevent the particles from moving further than one cell during a time step. Adequacy of the cell size was then determined from the particle trajectory. The length of a cell, L, could be determined by the Courant requirement, $L \geq U_{\max}\Delta t \approx 0.2075$.[35] This was estimated given that $\Delta t = 0.05$ in the particle output file and $U_{\max} \approx 4.15$ m s^{-1} in the freestream. The designated cell length scale, $L = 4$ m, was well above this limit.

Particles were released for approximately 20,000 time steps (1000 s) before the time-averaged concentration field was computed to allow the concentration of particles in the vicinity of the building array to reach a steady state. Additionally, this time allowed the velocity field to evolve into periodic vortex shedding and move through a sufficient number of cycles so that average velocity characteristics approached those at infinite time. The Strouhal number, *Str*, was used as a guide to estimate the expected dimensionless frequency of vortex shedding:

$$Str = \frac{fD}{u_\infty}, \tag{6}$$

where f is vortex shedding frequency, D is the characteristic dimension of the bluff body, and u_∞ is freestream velocity. Estimating *Str* to be 0.13 for a three-dimensional block structure[36] and with $u_\infty = 4.15$ m s^{-1} and the building height of 12 m as the characteristic dimension, approximately 45 shedding cycles should have evolved during the 1000 s before the concentration was first calculated.

For the concentration decay testing, the concentration field was computed for an additional 80 s, and instantaneous concentrations were then plotted as a function of time. In this case, concentration was averaged over two $2.6H \times 4H \times H$ regions within the source canyon lee of the tower and lee of the residential building centered at $y = -2.5H$.

Results and discussion

The results from the wind tunnel and CFD simulations of pollutant dispersion in this model urban neighborhood show a very significant impact of an isolated tower within an otherwise regular array of low buildings. Fig. 4 contains photographs from smoke visualization of the flow in the wake of the tower (Fig. 4a) and for the same building array geometry with the tower removed (Fig. 4b). For these photographs, theatrical smoke was emitted from a line source in the center of Avenue B and illuminated with a vertical laser light sheet centered on the tower building. Fig. 4a illustrates the upward vertical flow on the leeward face of the tower that is responsible for bringing the smoke (pollutants) up out of the street canyon and over the tops of the downwind buildings. The case without the tower (Fig. 4b) shows that the smoke remains more confined to the street canyons, and relatively little smoke escapes above the rooflines of the buildings. These findings were consistent with dispersion patterns observed by other researchers.[16,22,27,28]

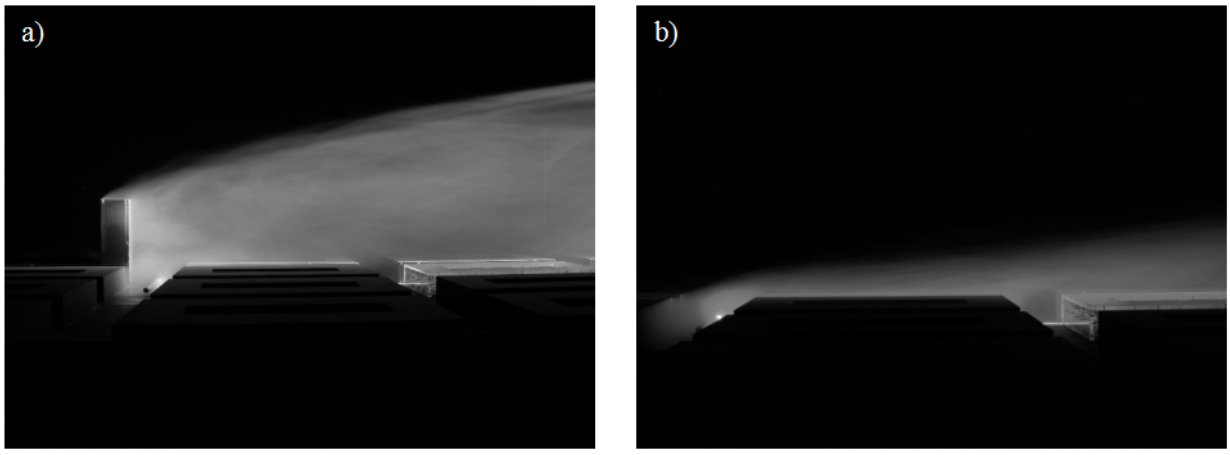

Fig. 4 Flow visualization, smoke illuminated with vertical laser light sheet, a) with tower and b) without tower.

Time-averaged concentration data

Individual line source segments. Concentration measurements were performed in the wind tunnel while releasing tracer gas from a line source located within a street canyon oriented perpendicular to the wind direction. Fig. 5 shows the time-averaged tracer gas concentration isopleths in Avenue B (the source street canyon) of the model. The line source was positioned in the center of the street canyon longitudinally and moved to three different positions laterally (as illustrated in Fig. 1). Measurements were made 0.67*H* downwind of the source, or half-way between the source and the downwind buildings. Fig. 6 shows the time-averaged tracer gas concentration isopleths in Avenue C for the same three source locations. Measurements were made along the centerline of the avenue.

Two interesting effects of the tower on the plume are the lateral movement towards the tower and the lifting of the plume in the wake of the tower. The plume from the source farthest from the tower is much wider than the plume from the source that is in front of the tower. This is caused by significant lateral flow towards the tower in these two street canyons (Avenues B and C), which can be seen very clearly in the velocity vectors presented in Heist *et al.*[11] In Avenue B, the height of the plume in the wake of the tower is about 6*H*, whereas the height of the plume two or three buildings over is only about 2*H*. In Avenue C, the height of the plume in the wake of the tower is about 7*H*, whereas the height of the plume two or three buildings over is only about 4*H*. The upwash on the downstream side of the tower is also shown in the velocity vectors presented in Heist *et al.*[11]

"Infinite" line source. Time-averaged concentration results for the infinite line source (calculated from eqn. (3)) are presented in Fig. 7. It is clear that the presence of the tower greatly influenced the vertical dispersion of the tracer. In the source street canyon (Fig. 7a), the height of the plume downwind of the tower was more than twice the height of the plume downwind of the buildings of unit height. The highest concentrations are seen in the intersections away from the tower and also in the wake of the tower. This demonstrates the upward vertical flow in the wake of the tower. Fig. 7b shows the infinite line source concentrations in the street canyon downwind of the source street. Again, the plume height was much greater in the wake of the tower than it was two or three blocks laterally.

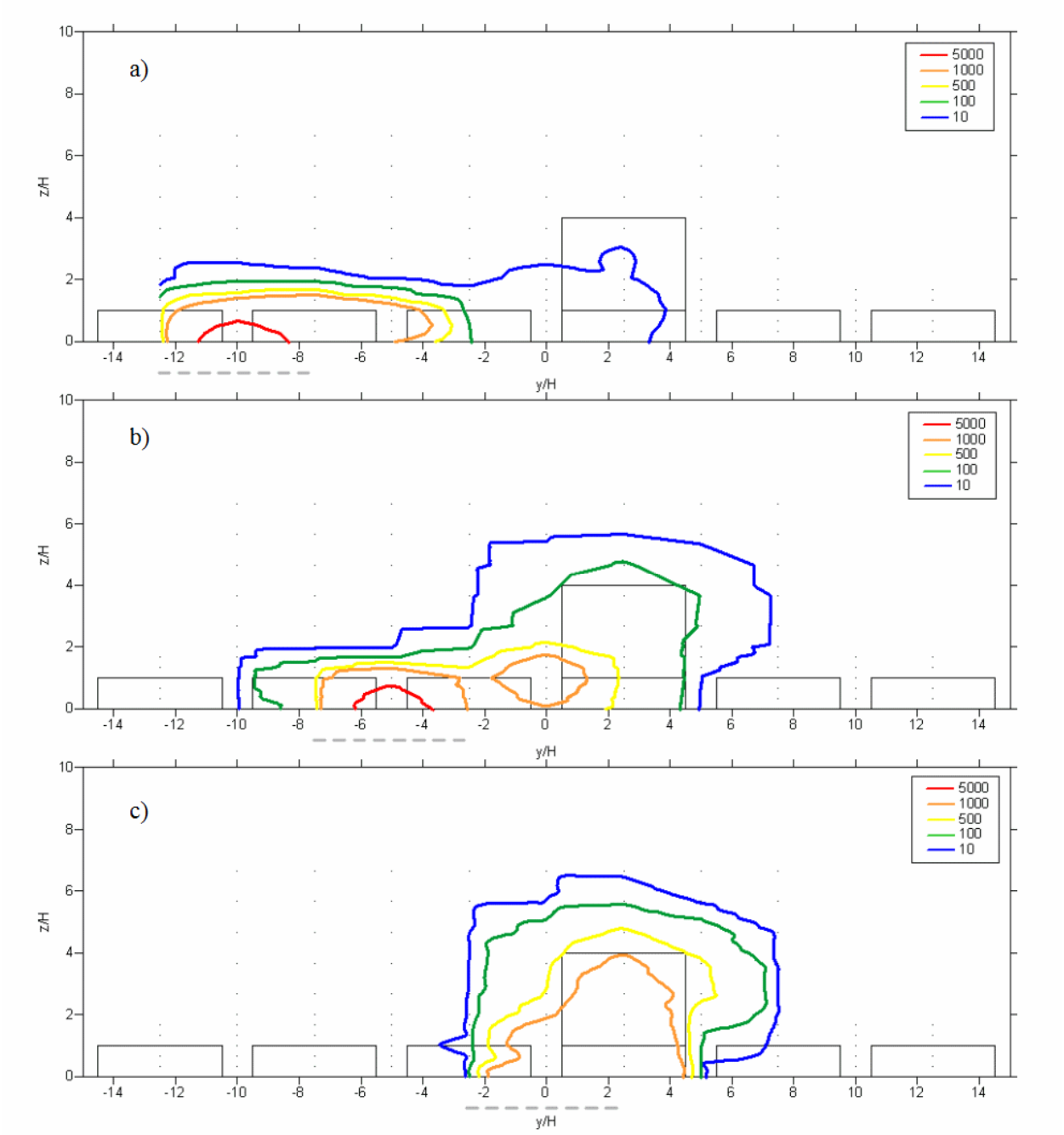

Fig. 5 MWT concentration in Avenue B (x = 0.67H) for source location a) S1, b) S2, and c) S3. Concentration represented as χ*1000. The dashed lines represent the source locations. The background dots show locations where concentration was measured. View looking upwind.

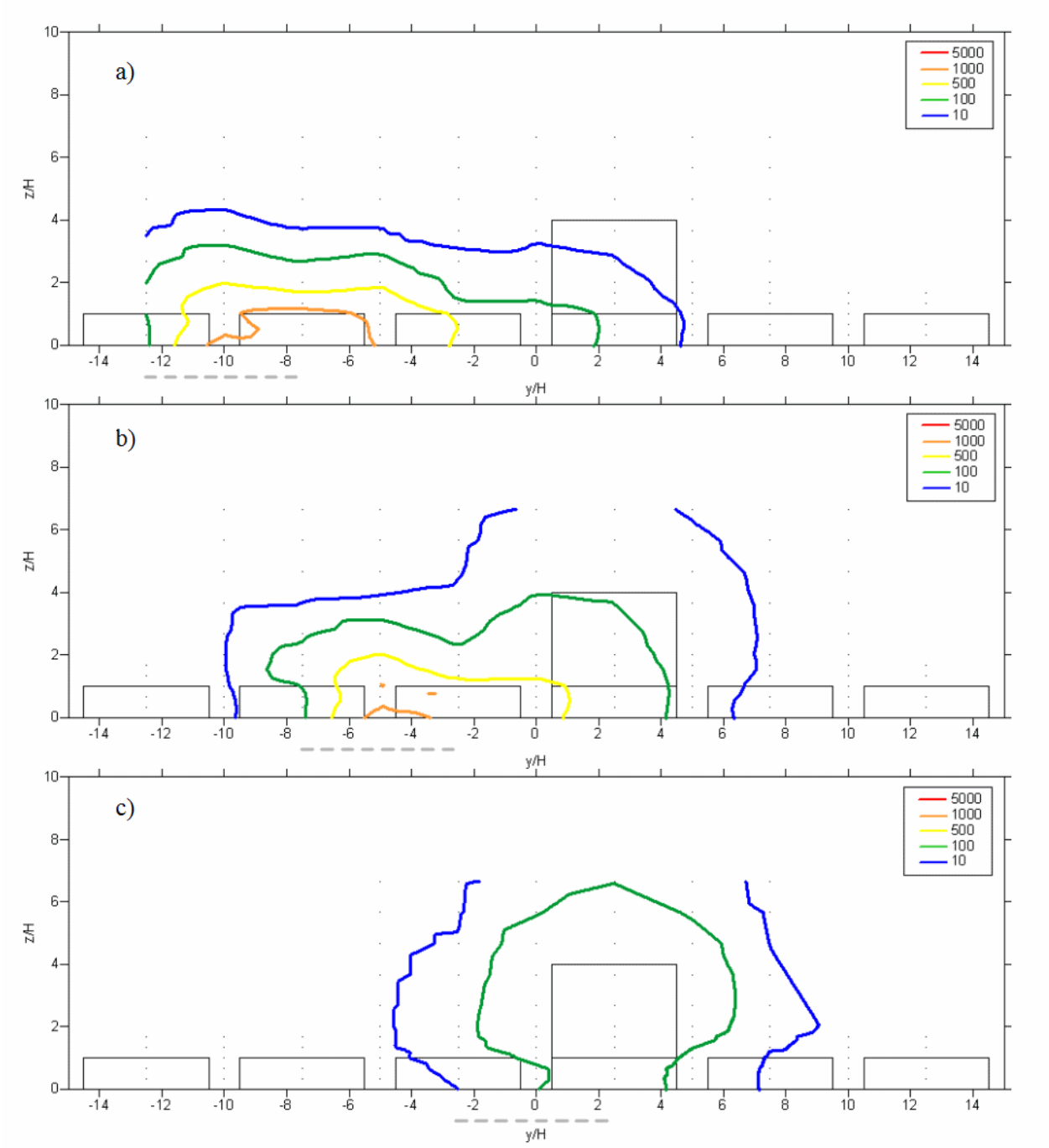

Fig. 6 MWT concentration in Avenue C (x = 10.3H) for source location a) S1, b) S2, and c) S3. Concentration represented as χ*1000. The dashed lines represent the source locations. The background dots show locations where concentration was measured. View looking upwind.

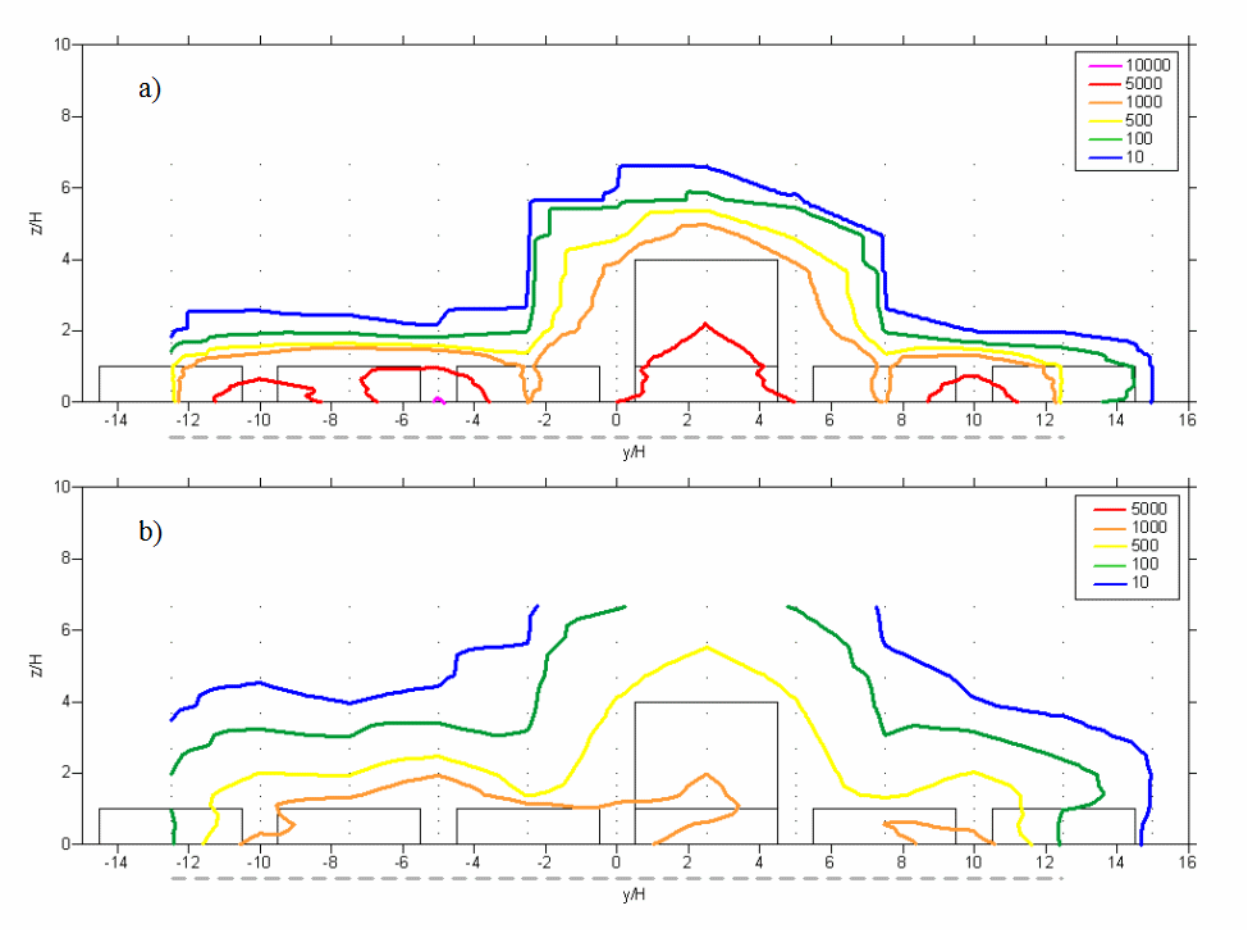

Fig. 7 "Infinite" line source construction of MWT concentration in a) Avenue B (x = 0.67H) and b) Avenue C (x = 10.3H). Concentration represented as χ*1000. The dashed lines represent the source locations. The background dots show locations where concentration was measured. View looking upwind.

The time-averaged results from CFD simulations are presented in Fig. 8. As mentioned earlier, the geometric models were somewhat different between the wind tunnel experiments and CFD modeling. The CFD model used fewer buildings (4 × 3 array *vs.* 6 × 5 array for the wind tunnel) and a slightly wider source street canyon (3H *vs.* 2.67H for the wind tunnel). Both models ran 120 s time averages. However, due to the scale of the wind tunnel model (1:100), the wind tunnel simulation would be equivalent to a CFD (full scale) 200 min average. Therefore, the wind tunnel concentration profiles appear smoother, whereas the CFD results look much more like an instantaneous sample.

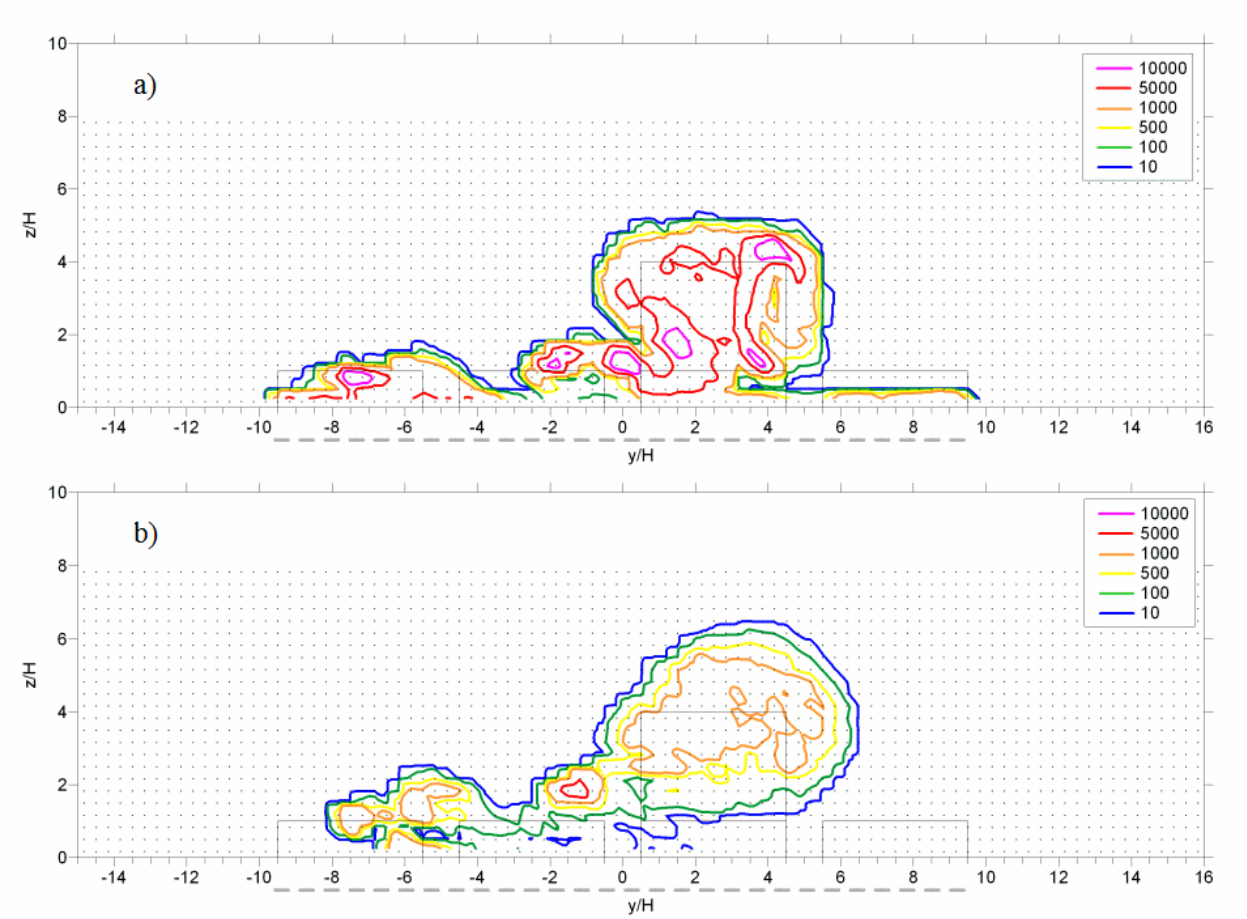

Fig. 8 CFD concentration in a) Avenue B (x = 0.5H) and b) Avenue C (x = 10.5H). Concentration represented as χ*1000. The dashed lines represent the source locations. The background dots show locations where concentration was calculated. View looking upwind.

There were several notable differences in the concentration patterns when comparing the wind tunnel and CFD results (Figs. 7 and 8). In both Avenue B and Avenue C, the plume material tended to reach greater heights in the wind tunnel. This was most pronounced in Avenue C (Figs. 7b and 8b). Both models displayed very high concentrations along the lee face of the tower. The CFD model, however, did not predict the very high concentrations seen in the intersections of Avenue B with the alongwind streets. It is possible that this discrepancy was caused by differences in the modeled flow in the alongwind streets adjacent to the block downwind of the tower. As shown by Heist *et al.*,[11] the CFD model predicted significant flow in the upwind direction in these alongwind street canyons directly in the wake of the tower, which

would act to pull air with lower pollutant levels from Avenue C to Avenue B. The wind tunnel simulations, on the other hand, showed significantly less flow reversal. There was also an asymmetry in the concentration pattern in the CFD model (Fig. 8), where there was little to no pollutant present to the right of the tower below $z = 1H$, that was not matched in the wind tunnel (Fig. 7). This was likely due to the difference in the size of the building array used for each model (4 blocks wide in the CFD model *vs.* 6 blocks in the wind tunnel), and therefore the decreased amount of source material available on that side of the tower in the CFD model.

Two-dimensional street canyons with the upwind building taller than the downwind building have been investigated using CFD simulations.[22,27] Both of these studies showed enhanced vertical dispersion in the wake of a taller building upwind of a shorter building, reinforcing our findings that the presence of a tall building enhances vertical dispersion downwind. Perry *et al.*,[29] who describe a three-dimensional model with isolated buildings significantly taller than the surrounding buildings, saw significant upwash in the lee of tall buildings in the model. Therefore, the upward advection of the plume in the wake of the tower in this study was not surprising. The influence of the tower on lateral flow in the street canyons (perpendicular to the wind direction) was significant in its ability to affect the dispersion of pollutants from a source several blocks away.

Concentration decay

CFD results. To illustrate the decay of pollutant concentration in the street canyon, CFD results are presented in Fig. 9 for the pollutant decay simulations. Concentrations are shown at $x/H = -0.16$, just upstream from the source canyon center, 10 s and 80 s after the source was shut off. As expected, the concentration decreased in the 70 s that elapsed between the two instantaneous concentration patterns shown in Fig. 9. There was very little pollutant to the right of the tower, as was also seen in Fig. 8. This may again be explained by the difference in the size of the building array used for each model and the decreased amount of source material available on that side of the tower.

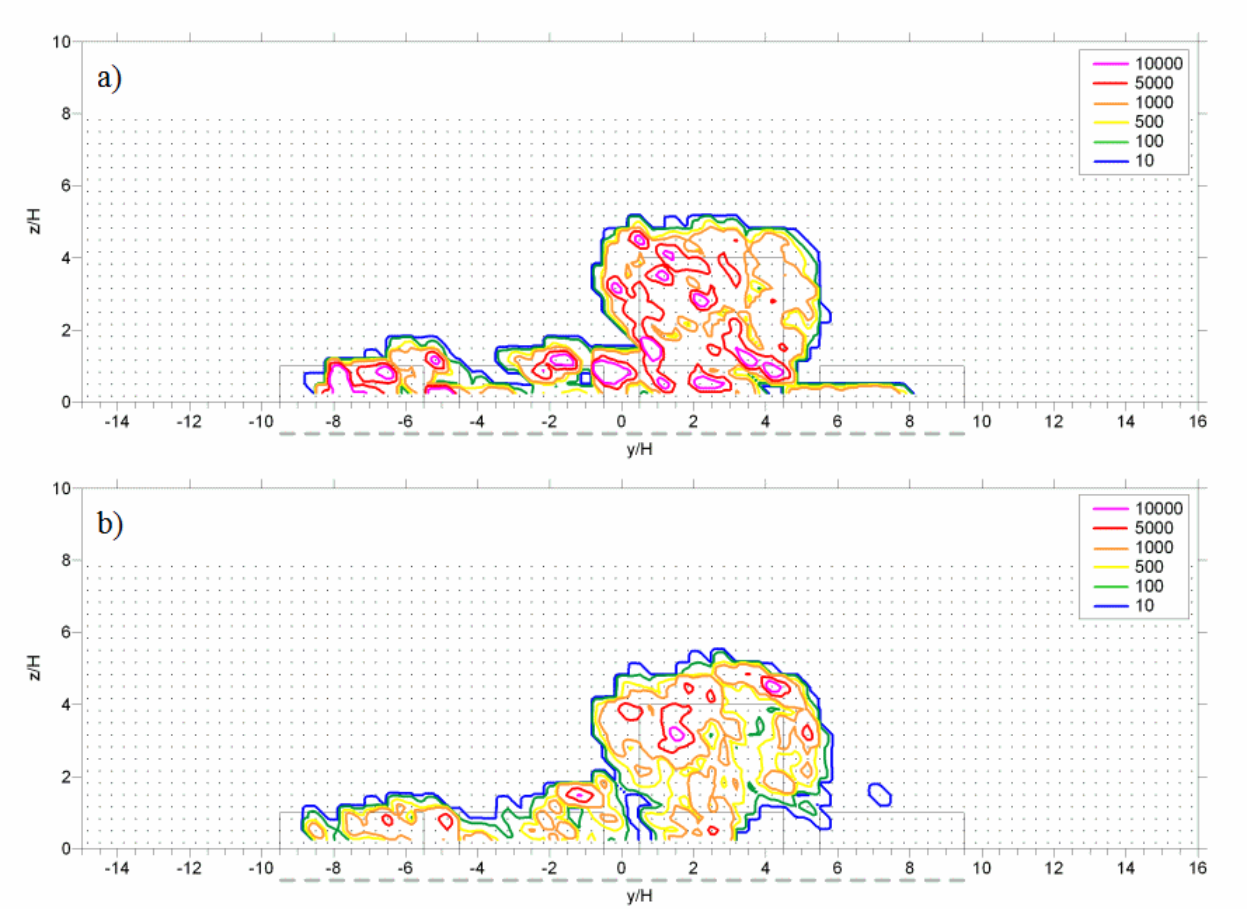

Fig. 9 CFD concentration in Avenue B (x = -0.16H) a) 10 s and b) 80 s after the source was turned off. Concentration represented as χ*1000. The dashed lines represent the source locations. The background dots show locations where concentration was calculated. View looking upwind.

To calculate the residence time, the average non-dimensionalized concentration (χ) in each of two zones was computed and plotted against time. The decay zones were located lee of the tower ($-1.3 \leq x/H \leq 1.3$, $0.5 \leq y/H \leq 4.5$, $z/H \leq 1$) and lee of a building with no tower ($-1.3 \leq x/H \leq 1.3$, $-4.5 \leq y/H \leq -0.5$, $z/H \leq 1$). Non-dimensionalized concentration as a function of time in each of these zones is shown in Fig. 10.

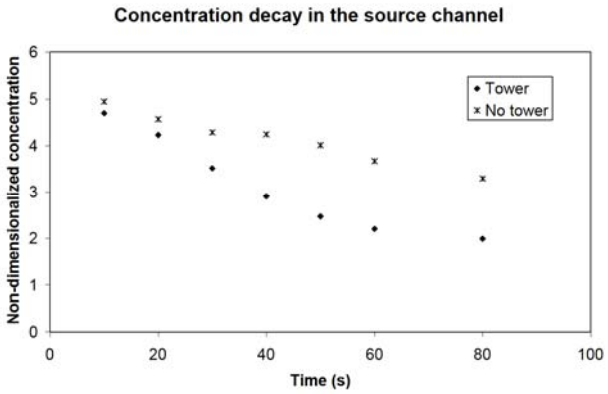

Fig. 10 Non-dimensionalized concentration (χ) *vs.* time for section of Avenue B ♦ lee of the tower ($-1.3 \le x/H \le 1.3$, $0.5 \le y/H \le 4.5$, $z/H \le 1$) and * lee of the unit-height building ($-1.3 \le x/H \le 1.3$, $-4.5 \le y/H \le -0.5$, $z/H \le 1$).

In dilution problems of this type, a reasonable first assumption is that, in the absence of any sources, the rate of change of χ will be linear and decreasing with time:

$$\frac{d\chi}{dt} = -\lambda\chi\,, \tag{7}$$

where λ is some rate constant, which can be expressed in terms of a time constant, τ, as $\lambda = 1/\tau$. Integration of eqn. (7) yields an exponential decay equation:

$$\chi(t) = A \cdot \exp(-t/\tau), \tag{8}$$

where A is a constant. The time constant, τ, is the characteristic residence time of the street canyon. This is consistent with the observations of Sini *et al.*[37] Eqn. (8) was fitted to the curves shown in Fig. 10. For the portion of the street canyon lee of the building of unit height, the best-fit equation was $\chi = 5.18 \cdot \exp(-0.0056t)$, and therefore $\tau = 178.6$ s. For the portion of the street canyon lee of the tower, the best-fit equation was $\chi = 5.22 \cdot \exp(-0.0133t)$, and therefore $\tau = 75.2$ s. This decrease of 58% when comparing the residence time downwind of the tower to that downwind of a unit height building demonstrated that the tower enhanced ventilation of the downwind street canyon.

Wind tunnel results for cubical blocks. The results of the concentration decay measurements for the array of cubical blocks in the wind tunnel are presented here. The time-dependent concentration data for 40 individual runs were averaged, and the residence time was calculated as described above for the CFD results. The best-fit equations for the four scenarios were as follows:

$$\begin{aligned} 1H.....C &= 0.5361 \cdot \exp(-1.5558t) \\ 1.5H...C &= 0.5679 \cdot \exp(-1.5626t) \\ 2H.....C &= 0.7835 \cdot \exp(-1.7856t) \\ 3H.....C &= 0.9042 \cdot \exp(-1.9565t) \end{aligned} \quad (9)$$

Therefore, for the block of unit height, the residence time, τ, was 0.643 s; the residence times for the 1.5H, 2H, and 3H cases were 0.639 s, 0.560 s, and 0.511 s, respectively. Because the scales and aspect ratios of the buildings (blocks) in these two studies of concentration decay were so different, resulting residence times (τ) were normalized by the residence time for a building having the same shape and of unit height (τ_{1H}) to facilitate comparison of the results. Normalized residence times are plotted against normalized building height in Fig. 11 for the CFD simulations and the cubical blocks wind tunnel study.

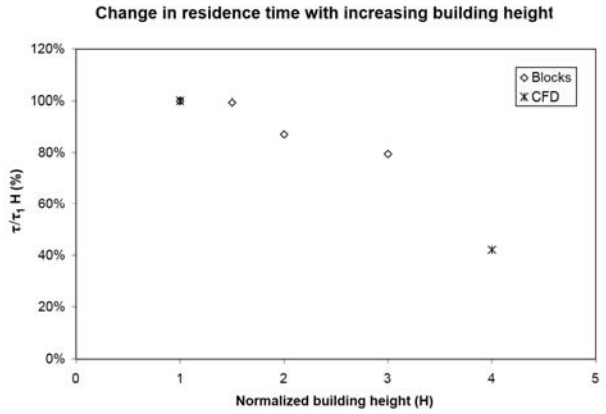

Fig. 11 Normalized residence time *vs.* building height for wind tunnel study with cubical blocks (◊) and CFD urban neighborhood study (*).

The results from this wind tunnel experiment and the CFD simulations above showed clearly that, with all other variables unchanged, the residence time in the canyon downwind of a taller block or building decreased with increasing height. Other factors such as building width and street canyon width likely play a role, but have not been examined here.

Conclusions

Pollutant dispersion in an idealized model urban neighborhood with one tall tower was studied using wind tunnel and CFD simulations. The results showed that the vertical dispersion of pollutants was greatly enhanced in the wake of the tall building. Three tower heights (12H)

downwind of the tower, the height of the plume was nearly twice the plume height in its absence. The tower also greatly enhanced lateral movement (towards the tower) in the street canyons, which was demonstrated by the increased plume width for sources further away from the tower laterally. The presence of the tower also significantly decreased the residence time of pollutants immediately downwind by 58% when compared to the residence time lee of a building of unit height.

References

1. M. Castillejos, V. H. Borja-Aburto, D. W. Dockery, D. R. Gold and D. Loomis, *Inhal. Toxicol.*, 2000, **12**(S1), 61–72.

2. D. W. Dockery, C. A. Pope, X. Xu, J. D. Spengler, J. H. Ware, M. E. Fay, B. G. Ferris and F. E. Speizer, *New Engl. J. Med.*, 1993, **329**, 1753–1759.

3. D. W. Dockery, *Environ. Health Perspect.*, 2001, **109**(S4), 483–486.

4. D. Krewski, R. T. Burnett, M. Goldberg, K. Hoover, J. Siemiatycki, M. Abrahamowicz and W. White, *Inhal. Toxicol.*, 2005, **17**, 335–342.

5. R. Maynard, *Sci. Total Environ.*, 2004, **334–335**, 9–13.

6. A. Monzón and M. J. Guerrero, *Sci. Total Environ.*, 2004, **334–335**, 427–434.

7. Z. E. Drake-Richman, L. A. Brixey, S. Lee, C. R. Fortune, A. D. Eisner, J. Richmond-Bryant, I. Hahn, W. D. Ellenson and R. W. Wiener, Precision and accuracy tests of the TSI P-Trak real-time ultrafine particle counter, 2007, in review.

8. A. D. Eisner, J. Richmond-Bryant, I. Hahn, Z. E. Drake-Richman, L. A. Brixey, W. D. Ellenson and R. W. Wiener, Analysis of indoor air pollution trends and characterization of infiltration delay time using a cross-correlation method, 2007, in review.

9. A. D. Eisner, J. Richmond-Bryant, I. Hahn, Z. E. Drake-Richman, W. D. Ellenson and R. W. Wiener, Establishing a link between vehicular PM sources and PM measurements in urban street canyons, 2007, in review.

10. I. Hahn, et al., Brooklyn Traffic Real-Time Ambient Pollutant Penetration and Environmental Dispersion (B-TRAPPED) Study: design and analysis methodology, 2007, in review.

11. D. K. Heist, J. Richmond-Bryant, L. A. Brixey, G. E. Bowker, S. G. Perry and R. W. Wiener, The effect of a tall tower on flow and dispersion through a model urban neighborhood, Part 1. flow characteristics, 2007, in review.

12. J. Richmond-Bryant, I. Hahn, C. R. Fortune, C. E. Rodes, S. Lee, J. W. Portzer, R. Baldauf, M. Wheeler, J. Seagraves, M. Stein, Z. E. Drake-Richman, L. A. Brixey, A. D. Eisner, W. D. Ellenson and R. W. Wiener, The Brooklyn Traffic Real-Time Ambient Pollutant Penetration and Environmental Dispersion (B-TRAPPED) Study, 2007, in review.

13. J. Richmond-Bryant, A. D. Eisner, I. Hahn, C. R. Fortune, Z. E. Drake-Richman, L. A. Brixey, M. Talih, W. D. Ellenson and R. W. Wiener, Time-series analysis to study the impact of an intersection on dispersion along a street canyon, 2007, in review.

14. W. H. Snyder, Guideline for Fluid Modeling of Atmospheric Diffusion, EPA-600/8-81-009, US Environmental Protection Agency, Research Triangle Park, NC, 1981.

15. C. H. Liu and M. C. Barth, *J. Appl. Meteorol.*, 2002, **41,** 660–673.

16. C. H. Liu, D. Y. C. Leung and M. C. Barth, *Atmos. Environ.*, 2005, **39**, 1567-1574.

17. F. S. Lien and E. Yee, *Boundary-Layer Meteorol.,* 2004, **112,** 427–466.

18. J. Baker, H. L. Walker and X. Cai, *Atmos. Environ.*, 2004, **38**, 6883–6892.

19. C. H. Chang and R. N. Meroney, *J. Wind Eng. Indus. Aerodyn.*, 2003, **91**, 1141–1154.

20. I. N. Harman, J. F. Barlow and S. E. Belcher, *Boundary-Layer Meteorol.*, 2004, **113**, 387–409.

21. J. Pullen, J. P. Boris, T. Young, G. Patnaik and J. Iselin, *Atmos. Environ.*, 2005, **39**, 1049–1068.

22. E. S. P. So, A. T. Y. Chan and A. Y. T. Wong, *Atmos. Environ.*, 2005, **39**, 3573–3582.

23. A. Walton, A. Y. S. Cheng and W. C. Yeung, *Atmos. Environ.*, 2002, **36**, 3601–3613.

24. A. Walton and A. Y. S. Cheng, *Atmos. Environ.*, 2002, **36**, 3615–3627.

25. Y. H. Tseng, C. Meneveau and M. B. Parlange, *Environ. Sci. Technol.,* 2006, **40**, 2653–2662.

26. S. R. Hanna, S. Tehranian, B. Carissimo, R. W. MacDonald and R. Lohner, *Atmos. Environ.*, 2002, **36**, 5067–5079.

27. J. Xia and D. Y. C. Leung, *Atmos. Environ.*, 2001, **135**, 2033–2043.

28. R. N. Meroney, M. Pavageau, S. Rafailidis and M. Schatzmann, *J. Wind Eng. Indus. Aerodyn.*, 1996, **62**, 37–56.

29. S. G. Perry, D. K. Heist, R. S. Thompson, W. H. Snyder and R. E. Lawson, *Environ. Manager*, February 2004, 31–34.

30. H. P. A. H. Irwin, *J. Wind Eng. Indus. Aerodyn.*, 1981, **7**, 361–366.

31. R. W. MacDonald, R. F. Griffiths and D. J. Hall, *Atmos. Environ.*, 1998, **32**, 3845–3862.

32. M. Schatzmann and B. Leitl, *Atmos. Environ.*, 2002, **36**, 4811–4821.

33. D. K. Heist, L. A. Brixey, S. G. Perry and G. E. Bowker, The effect of tall buildings on residence times in arrays of buildings, in Proceedings of PhysMod 2005—International Workshop on Physical Modeling of Flow and Dispersion Phenomena, London, ON, Canada, August 24-26, 2005, pp. 18-19.

34. R. J. Heinsohn, *Industrial Ventilation: Engineering Principles*, John Wiley & Sons, New York, NY, 1991.

35. P. J. Roache, *Verification and Validation in Computational Science and Engineering,* Hermosa Publishers, Albuquerque, NM, 1998.

36. M. Ozgoren, *Flow Meas. Instrum.*, 2006, **17**, 225–235.

37. J-F. Sini, S. Anquentin and P. G. Mestayer, *Atmos. Environ.*, 1996, **30**, 2659–2677.